

LEARNING A WARPED SUBSPACE MODEL OF FACES WITH IMAGES OF UNKNOWN POSE AND ILLUMINATION

Jihun Hamm and Daniel D. Lee

GRASP Laboratory, University of Pennsylvania, 3330 Walnut Street, Philadelphia, PA, USA

Keywords: Image-based modeling, probabilistic generative model, illumination subspace, super-resolution, MAP estimation, multiscale image registration.

Abstract: In this paper we tackle the problem of learning the appearances of a person's face from images with both unknown pose and illumination. The unknown, simultaneous change in pose and illumination makes it difficult to learn 3D face models from data without manual labeling and tracking of features. In comparison, image-based models do not require geometric knowledge of faces but only the statistics of data itself, and therefore are easier to train with images with such variations. We take an image-based approach to the problem and propose a generative model of a warped illumination subspace. Image variations due to illumination change are accounted for by a low-dimensional linear subspace, whereas variations due to pose change are approximated by a geometric warping of images in the subspace. We demonstrate that this model can be efficiently learned via MAP estimation and multiscale registration techniques. With this learned warped subspace we can jointly estimate the pose and the lighting conditions of test images and improve recognition of faces under novel poses and illuminations. We test our algorithm with synthetic faces and real images from the CMU PIE and Yale face databases. The results show improvements in prediction and recognition performance compared to other standard methods.

1 INTRODUCTION

We tackle the problem of learning generative models of a person's face from images with *both unknown pose and illumination*. The appearance of a person's face undergoes large variations as illumination and viewing directions change. A full 3D model of a face allows us to synthesize images at arbitrary poses and illumination conditions. However, learning such a 3D model from images alone is very difficult since it requires that feature correspondences are known accurately, even under dramatic lighting changes. In this paper we develop an image-based approach, which does not use 3D models nor solve correspondence problems, but instead directly learns the statistical properties of images under pose and illumination variations. (see Fig. 1).

One of the simplest image-based models of faces is an Eigenface model (Turk and Pentland, 1991), which models data as an affine subspace in the space of pixel intensities. Although Eigenfaces were originally applied to image variations across different peo-



Figure 1: Typical unlabeled images with both varying pose and illumination conditions make it difficult to learn 3D structures directly from sample images. We aim to learn an appearance model of a person's face given such images without finding, labeling and tracking features between frames.

ple, a subspace model can explain the illumination variation of a single person exceptionally well (Hallinan, 1994; Epstein et al., 1995). The so-called illumination subspace has been thoroughly studied theoretically (Ramamoorthi, 2002; Basri and Jacobs, 2003). However, such a linear subspace model cannot cope with the simultaneous nonlinear change of poses.

On the other hand, suppose we are given multiple-pose views of a face under a fixed lighting condition.

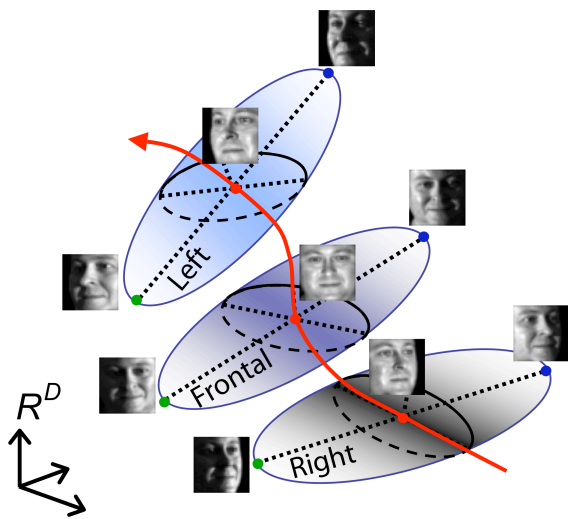


Figure 2: A probabilistic model of pose and illumination variations. The ellipsoid in the middle represents frontal images with all possible illuminations, lying closely on a low-dimensional subspace. As the viewpoint changes from a right-profile to a left-profile pose, the ellipsoid is transported continuously along a nonlinear manifold. We model this nonlinear variation with a geometric warping of images.

If the pose change is moderate, we can learn a generative model by geometrically registering the multi-view images and probabilistically combining them to estimate the unknown latent image. Such generative models have been proposed for the super-resolution problem (Hardie et al., 1997; Tipping and Bishop, 2002; Capel and Zisserman, 2003). However, previous work considers only a single latent image rather than a latent subspace, and therefore can handle only one-dimensional illumination changes and not the full range of illumination variations from arbitrary light sources.

In this paper we model the simultaneous change of pose and illumination of a person's face by a novel "warped subspace model." Image variations due to illumination change at a fixed pose are captured by a low-dimensional illumination subspace; and variations due to pose change are approximated by a geometric warping of images in the subspace. A schematic of the warped subspace is depicted in Fig. 2.

1.1 Related Work

Image-based models of faces have been proposed before. A popular multi-pose representation of images is the light-field presentation, which models the radiance of light as a function of the 5D pose of the observer (Gross et al., 2002a; Gross et al., 2002b; Zhou and Chellappa, 2004). Theoretically, the light-field

model provides pose-invariant recognition of images taken with arbitrary camera and pose when the illumination condition is fixed. Zhou et al. extended the light-field model to a bilinear model which allows simultaneous change of pose and illumination (Zhou and Chellappa, 2004). However, in practice, the camera pose of the test image has to be known beforehand to compare it with the pre-computed light-field, which effectively amounts to knowing the correspondence in 3D model-based approaches. This model is also unable to extend to the representation to a novel pose.

In the super-resolution field, the idea of using latent subspaces in generative models has been suggested by (Capel and Zisserman, 2001; Gunturk et al., 2003). However the learned subspaces reflect mixed contributions from pose, illumination, subject identities, etc. In our case the subspace encodes 3D structure, albedo and the low-pass filtering nature of the Lambertian reflectance function (Basri and Jacobs, 2003), and the pose change is dedicated to geometric transforms. Furthermore, we show how to learn the basis, pose and illumination conditions directly and simultaneously from a few images of *both unknown pose and illumination*. In our method we estimate the geometric warping variable via a continuous optimization instead of searching over a limited or finite set of predefined transformations (Hardie et al., 1997; Frey and Jojic, 1999; Tipping and Bishop, 2002).

The remainder of the paper is organized as follows. In Sec. 2, we formulate the warped subspace model in a probabilistic generative framework, and describe how to jointly estimate the pose and the illumination with a known basis. In Sec. 3, we describe a *maximum a posteriori* (MAP) approach to the learning of a basis as well as the estimation of pose and illumination simultaneously, and explain how a prior distribution and efficient optimization can be employed to learn the model. In Sec. 4, we perform recognition experiments on real data sets. We conclude with discussions in Sec. 5.

2 JOINT ESTIMATION OF POSE AND ILLUMINATION

In this section we explain the elements of generative models of images and optimization techniques to jointly estimate pose and illumination.

2.1 Generative Model of Multi-view Images

A simple generative model common to super-resolution methods is the following:

$$x = W_g z + \varepsilon, \quad (1)$$

where x is an observed image, z is a latent image, and W_g is a warping operator on the latent image: let $z(u, v)$ be the pixel intensity at $(u, v) \in \mathcal{R}^2$ and $T_g: \mathcal{R}^2 \rightarrow \mathcal{R}^2$ be a transform of coordinates parameterized by g , then

$$(W_g z)(u, v) = z(T_g^{-1}(u, v)).$$

In the finite-pixel domain, we assume x and z are D -dimensional vectors of image intensities where D is the number of pixels, and W_g is a $D \times D$ matrix representing the warping and the subsequent interpolation. From the definition above, the W_g is a nonlinear function of warping variables g ; however, it is a *linear* function of images z , which can be seen by the equality $W_g(a_1 I_1 + a_2 I_2) = a_1 (W_g I_1) + a_2 (W_g I_2)$, for any two images I_1 and I_2 and real numbers a_1 and a_2 .

We consider the perspective transforms in this paper, so g is a 8-dimensional vector. The $X = \{x_1, \dots, x_N\}$ and $G = \{g_1, \dots, g_N\}$ denote aggregates of N observed images and N warping variables.

If the noise ε is an independent, additive Gaussian noise, that is $p(x|z, g) \sim \mathcal{N}(W_g z, \Psi)$, then the log-likelihood of the observed samples X becomes

$$\begin{aligned} L &= \log p(X|z, G) = \sum_i \log p(x_i|z, g_i) \\ &= -\frac{1}{2} \sum_i (x_i - W_{g_i} z)' \Psi^{-1} (x_i - W_{g_i} z) \end{aligned} \quad (2)$$

plus a constant. The maximum likelihood (ML) estimates of the latent image z and the warping parameters G are found by computing

$$\operatorname{argmin}_{z, G} \sum_i (x_i - W_{g_i} z)' \Psi^{-1} (x_i - W_{g_i} z).$$

2.2 Warped Illumination Subspace

The previous model (1) can only explain the change of appearance from a single latent image. Instead, we want z to be a combination of basis images $z = Bs$, where B is a $D \times d$ matrix and s is d -dimensional vector and $d \ll D$. Our choice of B comes from the low-dimensional nature of illumination subspaces of convex Lambertian objects: an image illuminated from arbitrary light source distribution can be approximated well by a combination of four or nine-dimensional basis (Basri and Jacobs, 2003). In this

setting, B encodes 3D structure, albedo and the low-pass filtering nature of Lambertian reflectance, and the variables s determine the distribution of light sources. Let us call s illumination coefficients.

The corresponding generative model is

$$x = W_g B s + \varepsilon. \quad (3)$$

Since the warping W_g is a *linear* transform of images, the W_g maps a subspace to another subspace. In this sense we call our model a warped subspace model (refer to Fig. 2).

2.3 Optimization

Given an ensemble of images of the same object with unknown illumination and pose, we can learn g_i and s_i by minimizing the ML cost:

$$\begin{aligned} C &= -2 \log p(X|B, S, G) \\ &= \sum_i \|x_i - W_{g_i} B s_i\|_{\Psi}^2. \end{aligned} \quad (4)$$

We will use the notation $\|y\|_{\Psi}^2$ to denote the quadratic form $\|y\|_{\Psi}^2 = y' \Psi^{-1} y$. In super-resolution approaches, the warping variables g_i are typically computed once in a preprocessing step. Since we are dealing with images under arbitrary illumination change, a direct registration based on intensity is bound to fail. We overcome this problem by updating the registration variable g and illumination coefficient s in an alternating fashion.

2.3.1 Estimating Warping Variables g

To minimize (4) with respect to g we use a multi-scale registration technique (Vasconcelos and Lippman, 2005) to speed up computations and avoid local minima. At each level of coarse-to-fine image resolutions, registration is done by the Gauss-Newton method described in the following.

For simplicity assume the cost C is the sum of squared differences of two images I_1 and I_2

$$C = \sum_{u, v} [I_1(u, v) - I_2(T_g^{-1}(u, v))]^2. \quad (5)$$

The Gauss-Newton method finds the minimum of (5) by the update rule:

$$g^{n+1} = g^n - \alpha (\nabla_g^2 C|_{g^n})^{-1} \nabla_g C|_{g^n}, \quad (6)$$

where $\nabla_g C$ and $\nabla_g^2 C$ are the gradient and the Hessian of C , respectively. These are computed from the first- and the second-order derivatives of T with respect to g , and the first- and the second-order derivatives of images with respect to the coordinates (u, v) .

To apply the technique, we first generate image pyramids for I_1 and I_2 , we update g by (6) at the coarsest level of the pyramids until convergence, and repeat the iteration at the finer levels.

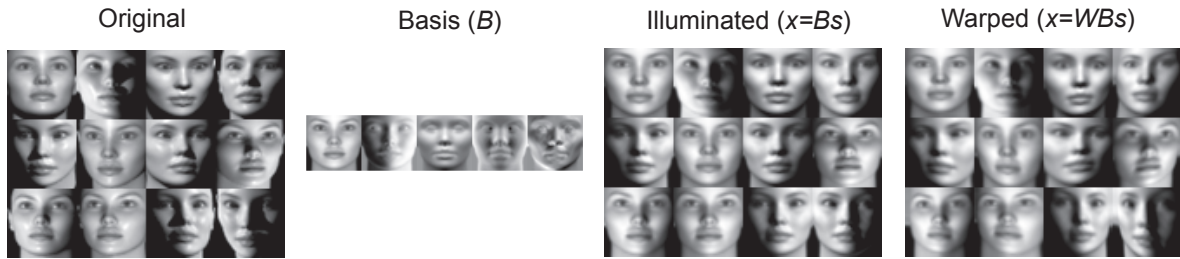


Figure 3: Modeling pose and lighting changes with a warped subspace model. By estimating the illumination coefficients s and the warping variables g with a known basis B , we can imitate the original pose and lighting on the left by the linear combination ($x = Bs$) followed by the geometrical warping ($x = W_gBs$).

2.3.2 Estimating Illumination Coefficients s

Minimizing the cost (4) with respect to s is straightforward. By setting

$$\frac{\partial \mathcal{C}}{\partial s_i} = 2B'W_i'\Psi^{-1}(W_iBs_i - x_i) = 0$$

we get the linear equation

$$(B'W_i'\Psi^{-1}W_iB)s_i = B'W_i'\Psi^{-1}x_i, \quad (7)$$

which can be directly solved by inverting $d \times d$ matrix. Note that $d \ll D$.

2.4 Experiments with Synthetic Data

We test the alternating minimization scheme with synthetic face data. For this purpose, we first generated synthetic images from a 3D model of a person with a fixed pose and varying illuminations, from which an empirical basis B is computed by singular value decomposition (SVD). The number of basis vector $d = 5$ was chosen to contain more than 98.8 percent of the total energy, which agrees with empirical (Epstein et al., 1995) and analytical (Ramamoorthi, 2002) studies.

A number of images were randomly rendered with varying pose ($|\text{yaw}| \leq 15^\circ, |\text{pitch}| \leq 12^\circ$) and varying light source direction ($|\text{yaw}| \leq 60^\circ, |\text{pitch}| \leq 50^\circ$). The noise statistics Ψ were manually determined from the statistics of the error between the true and the reconstructed images. Figure 3 shows the basis images and the result of joint estimation.

3 SIMULTANEOUS LEARNING OF BASIS

In the previous section we showed how to jointly estimate pose and lighting conditions of test images from

a known basis. However, in practice we do not know the basis for a given person beforehand. In this section we demonstrate an efficient method of learning the basis as well.

3.1 MAP Estimation

By considering B also as an unknown variable the ML cost (4) becomes certainly harder to minimize. The main difficulty lies in the degeneracy of the product WBs . First, the product Bs is degenerate up to matrix multiplications of any nonsingular matrix A , that is, $Bs = BA^{-1}As$. We will impose orthogonality on the basis $B'B = I$, but the B and s are still degenerate up to a $d \times d$ rotation matrix. Secondly, W and Bs are also degenerate. One can warp the basis by some transformation T and compensate it by its inverse: $WBs = WT^{-1}TBs$.

To relieve the difficulty, we assume a Gaussian process prior on B and a Gaussian density prior on g . These priors can break the degeneracy by preferring specific values of (W, B, s) among those which give the same value of WBs .

3.1.1 Gaussian Process Prior for Images

In super-resolution problems, finding latent images z is usually ill-posed and a prior is required for z . One of the commonly used priors is the Gaussian MRF (Capel and Zisserman, 2003) of the form $p(z) = \frac{1}{Z} \exp(-z'Qz)$, which can be viewed as a Gaussian random process prior on $z \sim \mathcal{N}(\mu, \Phi)$ whose covariance reflects the MRF properties.

We propose the following prior: if b_j denotes the j -th column of B , then each $\{b_j\}$ has the i.i.d. Gaussian prior $b_j \sim \mathcal{N}(\mu, \Phi)$. It is typical to assume $\mu_i = 0$ for all arbitrary images, but we can also use the empirical basis images, such as those from the previous experiments with synthetic faces. We further assume b_j 's are independent. For Φ we choose RBF co-

variance described in (Tipping and Bishop, 2002): if the i -th and j -th entries of z correspond to the pixels (u_i, v_i) and (u_j, v_j) in image coordinates, then $[\Phi]_{ij} \propto \exp\left(-\frac{1}{2r^2}\{(u_i - u_j)^2 + (v_i - v_j)^2\}\right)$. The inverse $Q = \Phi^{-1}$ of the RBF covariance penalize abrupt changes in the values of nearby pixels and act as a smoothness prior. In practice, the $Q = \Phi^{-1}$ need not be invertible, and can be made sparse to speed up computations. The independence assumption on the basis images $\{b_j\}$ may seem too restrictive, because the basis images $\{b_j\}$ may be correlated. However, the MRF prior serves mainly as the smoothness regularizer and the independence only implies that the basis images are independently smooth. Besides, assuming the full dependency of basis images is not practical due to the sheer size of the covariance matrix.

3.1.2 Regularized Warping

A prior for g can prevent unrealistic over-registration and make the problem better-posed. We penalized the L_2 norm of the displacement field. Suppose $(\delta u, \delta v) = T_g(u, v) - (u, v)$ is the displacement field of the transform T_g , then the norm $\sum_{(u,v)} (\delta u)^2 + (\delta v)^2$ measure the overall distortion the transform T_g induces. The second-order approximation to the squared norm around $g = 0$ is

$$\sum_{(u,v)} \{(\nabla_g \delta u)'g\}^2 + \{(\nabla_g \delta v)'g\}^2 = g' \Lambda g$$

The corresponding regularization term $\log p(g) = -\lambda g' \Lambda g$ is added to the registration error term (5) in our multiscale registration procedure. For perspective transforms, the Λ is a 8×8 matrix which doesn't depend on data.

3.2 Optimization

The proposed MAP cost is as follows:

$$\begin{aligned} \mathcal{C} &= -2 \log [p(X|B, S, G)p(B)p(G)] \\ &= \sum_i \|x_i - W_{g_i} B s_i\|_{\Psi}^2 + \lambda \sum_i g_i' \Lambda g_i \\ &\quad + \eta N \sum_j \|b_j - \mu_j\|_{\Phi}^2 + \text{const} \end{aligned} \quad (8)$$

The minimization is similarly done by alternating between minimizations over B , s and g . Minimizing over the latter two is the same as previous section, and we only describe minimization over B .

3.2.1 Finding Basis Images B

The derivative of \mathcal{C} w.r.t B is

$$\begin{aligned} \frac{\partial \mathcal{C}}{\partial B} &= 2 \sum_i W_i' \Psi^{-1} (W_i B s_i - x_i) s_i' \\ &\quad + 2\eta N \Phi^{-1} (B - \mu), \end{aligned}$$

where $\mu = [\mu_1 \dots \mu_d]$. An exact solution is given by setting $\frac{\partial \mathcal{C}}{\partial B} = 0$:

$$\sum_i W_i' \Psi^{-1} (W_i B s_i - x_i) s_i' + \eta N \Phi^{-1} (B - \mu) = 0. \quad (9)$$

We can solve the equation either directly or by a conjugate gradient method. After updating B , we orthogonalize it by a Gram-Schmidt procedure.

3.3 Algorithm

The final algorithm is summarized below:

1. initialize g , s and B .
2. for $i = 1, \dots, N$, minimize \mathcal{C} over g_i by multi-scale registration.
3. for $i = 1, \dots, N$, solve (7) for s_i by inversion.
4. solve (9) for B by scaled conjugate gradient.
5. orthogonalize B by Gram-Schmidt procedure.
6. repeat 2–5 until convergence.

4 APPLICATIONS TO FACE RECOGNITION

In this section we perform prediction and recognition experiments with real images from the Yale face and CMU-PIE databases.

4.1 Yale Face Database

The Yale face database (Georghiadis et al., 2001) consists of images from 10 subjects under 9 different poses and 43 different lighting conditions.¹ From the original images we roughly crop face regions and resize them to 40×40 images ($D = 1600$). Each image is then normalized to have the same sum-of-squares. All images are globally rescaled to have the min/max value of 0/1.

As a training set of each subject we randomly select two images with arbitrary lighting condition per pose, to get a total of $2 \times 9 = 18$ images of unknown

¹two of the lighting conditions ('A-005E+10' and 'A+050E-40') are dropped due to erroneous recording.

pose and illumination of the subject. The test set of each subject comprises all remaining images which are not in the training set ($43 \times 9 - 18 = 369$) of the subject. The 43 lighting conditions in the test set are divided into four subsets as explained in (Georghiadis et al., 2001) according to the angle the light source direction makes with the frontal direction. The four subsets consists of 6, 12, 12, and 13 lighting conditions respectively with increasing angles.

We generated multiple pairs of training/test sets to get averaged results from random choices of training set.

4.2 CMU PIE Database

The CMU-PIE database (Sim et al., 2003) consists of images from 68 subjects under 13 different poses and 43 different lighting conditions.

We arbitrarily chose the same number (=10) of subjects as the Yale face in our tests. Among 13 original camera poses, we have chosen 7 poses whose angles with the frontal camera pose are roughly less than 40° ,² and 21 lighting conditions without background lights. We similarly detect and crop face regions from the original data to a size of 40×40 and rescale the intensity.

As a training set of each subject we randomly select two images of arbitrary lighting condition per pose to get a total of $2 \times 7 = 14$ images of unknown pose and illumination of the subject. The test set of each subject comprises all remaining images which are not in the training set ($21 \times 7 - 14 = 133$) of the subject. We also divided the testing set into three subsets, according to the angle the light source direction makes with the frontal axis ($0 - 20^\circ$, $20 - 35^\circ$, $35 - 67^\circ$). The four subsets consists of 7, 6, and 8 lighting conditions respectively.

We also generated multiple pairs of training/test sets for CMU PIE.

4.3 Parameter Selection

In an earlier section we empirically determined the value of d and Ψ from synthetic data. Similarly, we manually chose the parameters $\{\lambda, \eta, \Phi\}$ by experimenting with synthetic faces. The λ relates to the amount of warping and $\{\eta, \Phi\}$ relates to the smoothness of images. As these parameters do not reflect the peculiarity of each person, we can the same values for the Yale face and CMU PIE database as the values for synthetic data without exhaustive fine-tunings.

²cameras numbered '05', '07', '09', '11', '27', '29', '37'

Table 1: Average prediction error $\|x - \hat{x}\|^2 / \|x\|^2$ of linear vs warped subspace models from the Yale face (upper) and and CMU PIE (lower) databases.

Subset #	1	2	3	4
Linear	0.0568	0.0676	0.1056	0.1837
Warped	0.0124	0.0154	0.0269	0.0609

Subset #	1	2	3
Linear	0.0887	0.1068	0.1535
Warped	0.0149	0.0174	0.0359

4.4 Prediction Results

We demonstrate the advantage of having a nonlinear warping to a linear subspace model in prediction. From 18 (and 14) images of a person from the Yale face (and CMU PIE) database, we learn the two sets of bases:

- **Linear subspace:** 5-dimensional basis B_{lin}^j is computed from SVD of the training data of j -th subject. The prediction \hat{x} is given by $\hat{x} = B_{\text{lin}}^j (B_{\text{lin}}^j)^t x$.
- **Warped subspace:** 5-dimensional basis B_{warp}^j , warping variable g^j , and light coefficients s^j are computed from the training data of j -th subject, by minimizing the MAP cost (8) iteratively from the initial value B_{lin}^j . The prediction \hat{x} is given by $\hat{x} = W_{g^j} B_{\text{warp}}^j s^j$.

Figure 4 shows sample results from the two methods.

Quantitative evaluations are performed as follows. Prediction error for each image is defined as the fractional error between true the image x and the predicted image \hat{x} : $\text{err} = \|x - \hat{x}\|^2 / \|x\|^2$ averaged over all test images. The result is shown in Table 1. Our method reduces the error to 16 ~ 33 percent of the error from the linear model.

4.5 Recognition Results

We compare recognition performance of our method with four other standard appearance-based methods suggested in (Georghiadis et al., 2001). These include the nearest-neighbor classifiers which do not use subject identity in training: correlation, eigenface, and eigenface without the first three eigenvectors. For these we have used 50 eigenvectors. The other two methods are the same as in the prediction experiments (linear subspace and warped subspace). The average recognition errors were computed over all con-

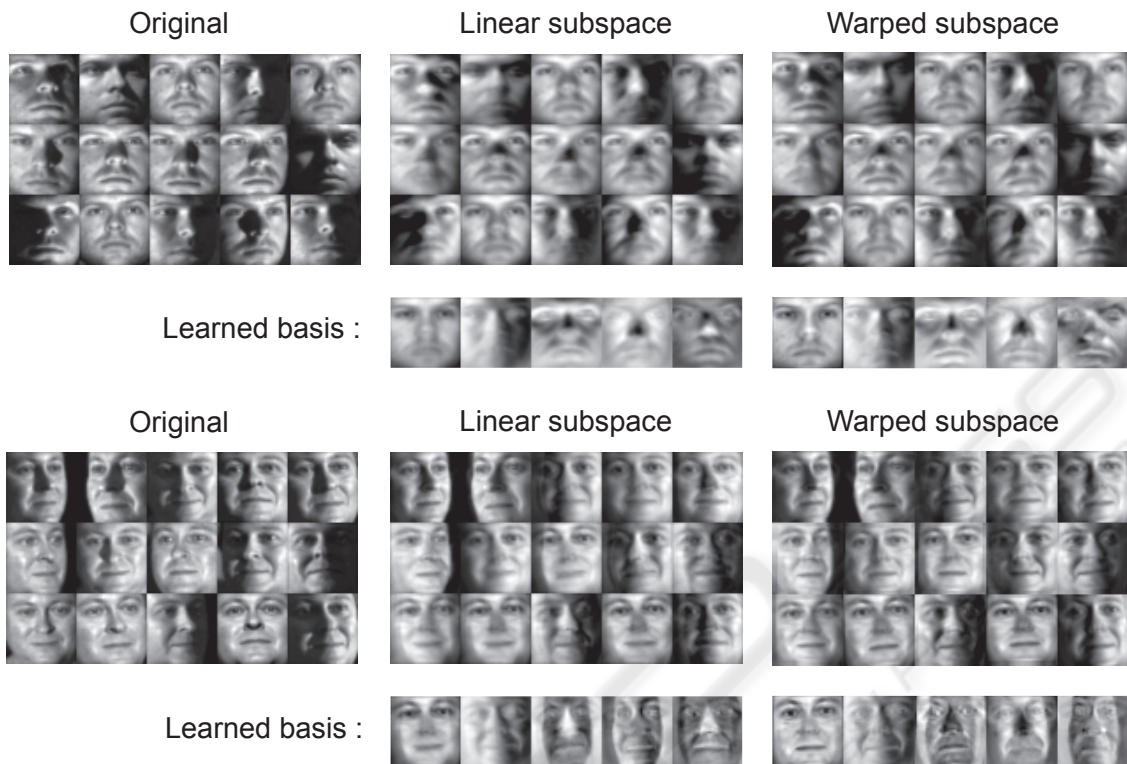


Figure 4: Experiments with the Yale face (upper) and CMU PIE (lower) databases. Reconstructions of the original images with a linear subspace model (middle) and with a warped subspace model (right) are compared along with the learned bases from the two methods. The warped subspace model shows increased resolutions and sharpness in the learned basis and the reconstructed images.

ditions and all subjects from Yale face and CMU PIE databases, shown in Fig. 5.

5 CONCLUSIONS

The Eigenface is an almost two-decade old subspace model. Still, it serves as a fundamental image-based model due to its simplicity. In this work we re-vamped the subspace model to a warped subspace model which can cope with both the linear variability in illumination and the nonlinear variability in pose. Given a few training images, the model can estimate the basis, pose and illumination conditions simultaneously via MAP estimation and multiscale registration technique. Experimental results confirm the advantage of the warped subspace model over the standard image-based models in prediction and recognition tasks. We are currently working on increasing the range of pose our model can handle.

REFERENCES

- Basri, R. and Jacobs, D. W. (2003). Lambertian reflectance and linear subspaces. *IEEE Trans. Pattern Analysis and Machine Intelligence*, 25(2):218–233.
- Capel, D. and Zisserman, A. (2003). Computer vision applied to super resolution. *IEEE Signal Processing Magazine*, 20(3):75–86.
- Capel, D. P. and Zisserman, A. (2001). Super-resolution from multiple views using learnt image models. In *CVPR*, volume 2, pages 627–634.
- Epstein, R., Hallinan, P., and Yuille, A. (1995). 5 ± 2 Eigenimages suffice: An empirical investigation of low-dimensional lighting models. In *Proceedings of IEEE Workshop on Physics-Based Modeling in Computer Vision*, pages 108–116.
- Frey, B. J. and Jovic, N. (1999). Transformed component analysis: Joint estimation of spatial transformations and image components. In *ICCV*, page 1190, Washington, DC, USA. IEEE Computer Society.
- Georghiades, A. S., Belhumeur, P. N., and Kriegman, D. J. (2001). From few to many: Illumination cone models for face recognition under variable lighting and

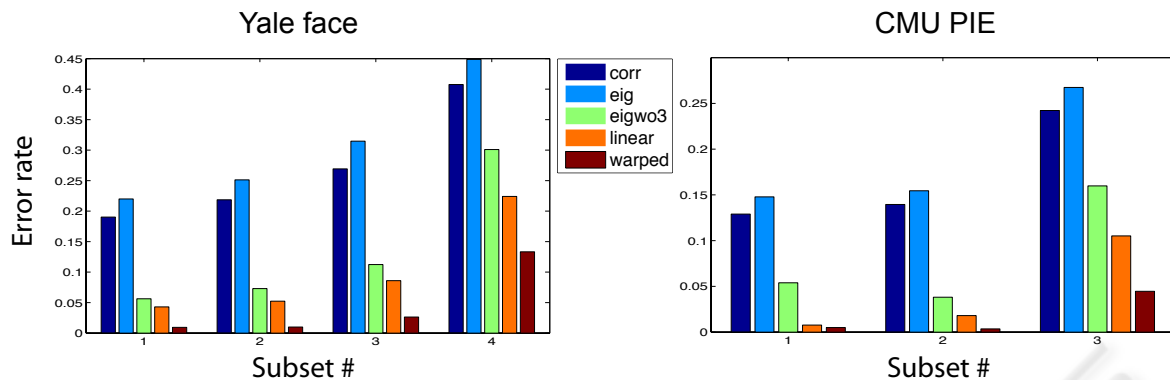


Figure 5: Average recognition error of five algorithms for the Yale face (left) and CMU PIE (right) databases. The warped subspace model achieves the smallest error across different test subsets of lighting variations.

- pose. *IEEE Trans. Pattern Analysis and Machine Intelligence*, 23(6):643–660.
- Gross, R., Matthews, I., and Baker, S. (2002a). Eigen light-fields and face recognition across pose. In *FGR '02: Proceedings of the Fifth IEEE International Conference on Automatic Face and Gesture Recognition*, page 3, Washington, DC, USA. IEEE Computer Society.
- Gross, R., Matthews, I., and Baker, S. (2002b). Fisher light-fields for face recognition across pose and illumination. In *Proceedings of the 24th DAGM Symposium on Pattern Recognition*, pages 481–489, London, UK. Springer-Verlag.
- Gunturk, B. K., Batur, A. U., Altunbasak, Y., III, M. H. H., and Mersereau, R. M. (2003). Eigenface-domain super-resolution for face recognition. *IEEE Trans. Image Processing*, 12(5):597–606.
- Hallinan, P. (1994). A low-dimensional representation of human faces for arbitrary lighting conditions. In *Proc. IEEE Conf. Computer Vision and Pattern Recognition*, pages 995–999.
- Hardie, R. C., Barnard, K. J., and Armstrong, E. E. (1997). Joint MAP registration and high-resolution image estimation using a sequence of undersampled images. *IEEE Trans. Image Processing*, 6(12):1621–1633.
- Ramamoorthi, R. (2002). Analytic PCA construction for theoretical analysis of lighting variability in images of a Lambertian object. *IEEE Trans. Pattern Analysis and Machine Intelligence*, 24(10):1322–1333.
- Sim, T., Baker, S., and Bsat, M. (2003). The CMU pose, illumination, and expression (PIE) database. *IEEE Trans. Pattern Analysis and Machine Intelligence*, 25(12):1615–1618.
- Tipping, M. E. and Bishop, C. M. (2002). Bayesian image super-resolution. In Becker, S., Thrun, S., and Obermayer, K., editors, *NIPS*, pages 1279–1286. MIT Press.
- Turk, M. and Pentland, A. P. (1991). Eigenfaces for recognition. *Journal of Cognitive Neuroscience*, 3(1):71–86.
- Vasconcelos, N. and Lippman, A. (2005). A multiresolution manifold distance for invariant image similarity. *IEEE Trans. Multimedia*, 7(1):127–142.
- Zhou, S. K. and Chellappa, R. (2004). Illuminating light field: Image-based face recognition across illuminations and poses. In *FGR*, pages 229–234. IEEE Computer Society.